Astrophysical Signatures of Konoplya-Zhidenko Black Holes: Gravitational Lensing and Thermodynamics

İzzet Sakallı

izzet.sakalli@emu.edu.tr

Eastern Mediterranean University

Erdem Sucu

Eastern Mediterranean University

Research Article

Keywords: Black holes, Deformed spacetime, Gravitational lensing, Quantum thermodynamics, Konoplya-Zhidenko metric

Posted Date: April 28th, 2025

DOI: https://doi.org/10.21203/rs.3.rs-6424840/v1

Additional Declarations: No competing interests reported.

Astrophysical Signatures of Konoplya-Zhidenko Black Holes: Gravitational Lensing and Thermodynamics

İzzet Sakallı [1,*] and Erdem Sucu [1,†]

[1] *Physics Department, Eastern Mediterranean University, Famagusta, 99628 North Cyprus, via Mersin 10, Turkiye*

(Dated: April 10, 2025)

This study investigates the astrophysical implications of deformed black hole geometries, specifically focusing on the Konoplya-Zhidenko (KZ) metric which introduces parametric deviations to the standard Schwarzschild solution. We analyze how the deformation parameter η modifies key physical properties across multiple domains: thermodynamic behavior, gravitational lensing characteristics, and quantum-corrected entropy. Our results demonstrate that even modest deviations from general relativity produce significant alterations in Hawking temperature profiles, event horizon structure, and black hole stability conditions. Through application of the GB theorem, we derive weak deflection angles in vacuum and plasma environments, revealing enhanced gravitational lensing effects particularly prominent at small impact parameters. The inclusion of exponential correction entropy formalism further elucidates how quantum modifications influence critical thermodynamic quantities including internal energy, Helmholtz free energy, and heat capacity. Additionally, using the Jacobi metric approach, we extend our analysis to massive particles, showing that velocity-dependent corrections to deflection angles emerge naturally from the deformed geometry. These findings collectively contribute to a more comprehensive understanding of modified gravity theories and establish a theoretical framework for empirical verification through high-precision astrophysical observations of black hole systems.

Keywords: Black holes; Deformed spacetime; Gravitational lensing; Quantum thermodynamics; Konoplya-Zhidenko metric

I. INTRODUCTION

Black holes (BHs) represent the quintessential astrophysical laboratories for investigating fundamental physical theories across extreme gravitational regimes. These enigmatic objects, characterized by their event horizons and gravitational singularities, continue to challenge our understanding of spacetime geometry, general relativity (GR), and quantum field theory in curved backgrounds [1–3]. Recent observational breakthroughs—including gravitational wave detections by LIGO-Virgo-KAGRA collaborations and the remarkable BH shadow imaging by the Event Horizon Telescope (EHT)—have transformed these formerly theoretical constructs into empirically accessible entities [4–6]. Despite these advances, significant questions persist regarding potential deviations from the standard Schwarzschild and Kerr metrics that might arise from quantum gravity effects, modified gravity theories, or exotic matter distributions.

The KZ metric offers a particularly valuable framework for systematically investigating parameterized deviations from classical GR solutions [7, 8]. This metric introduces modifications to the standard Schwarzschild spacetime through a power series expansion of the mass function, effectively parameterizing potential quantum gravity corrections while preserving asymptotic flatness. The primary advantage of the KZ approach lies in its model-independent characterization of deviations, which allows for systematic exploration of a broad class of modified gravity theories without commitment to specific theoretical frameworks. By introducing the deformation parameter η, which quantifies departures from the Schwarzschild solution, the static KZ (SKZ) metric enables a controlled investigation of how such modifications affect astrophysical observables [9, 10].

Gravitational lensing represents one of the most powerful probes of spacetime geometry and serves as a critical observational window into BH physics [11–16]. When light from distant sources traverses the vicinity of massive objects, the curved spacetime geometry induces deflection, amplification, and multiple imaging effects that carry distinctive signatures of the underlying gravitational field [17, 18]. Classical lensing theory, developed within the framework of GR, has achieved remarkable success in predicting and explaining observed phenomena around galaxies, galaxy clusters, and stellar-mass objects [19, 20]. However, the potential influence of modified gravity effects on lensing observables remains an active frontier of investigation. In the context of SKZ BHs, gravitational lensing serves as an ideal probe of the deformation parameter η, particularly in strong field regimes where deviations from GR become more pronounced [21, 22]. Calculating deflection angles constitutes a fundamental aspect of gravitational lensing analysis. Traditional approaches based on geodesic equations provide a direct connection between spacetime geometry and light propagation paths. In recent years, the application of topological methods, particularly the Gauss-Bonnet (GB) theorem, has emerged as a powerful alternative technique for calculating weak deflection an-

* izzet.sakalli@emu.edu.tr
† erdemsc07@gmail.com

gles [23–26]. This approach contextualizes the deflection phenomenon as a global topological effect rather than merely as a local geodesic property, offering computational advantages and conceptual insights. Our investigation employs both classical geodesic-based perturbative techniques and the GB approach, allowing for comprehensive cross-validation of results while highlighting the complementary aspects of these methodologies.

Magnification properties represent another critical dimension of gravitational lensing phenomena that carries distinguishing signatures of the underlying spacetime geometry [11, 27, 28]. When light bundles propagate through curved spacetime, they experience differential focusing and shearing that manifests as magnification or demagnification of source brightness [29]. For SKZ BHs, these effects are notably influenced by the deformation parameter η, which modifies the effective gravitational potential and consequently alters the convergence properties of light rays. The study of tangential and radial magnification components provides valuable insights into the formation of critical curves and caustic structures, which in turn determine the multiplicity and brightness of gravitationally lensed images. These magnification signatures offer potentially observable discriminants between standard GR BHs and their modified counterparts.

The presence of plasma in astrophysical environments introduces additional complexity to gravitational lensing phenomena [30, 31]. Unlike vacuum propagation, light rays traversing plasma media experience frequency-dependent refractive effects that couple with the underlying spacetime curvature to produce chromatic lensing signatures [32]. This plasma-gravity interaction manifests as frequency-dependent corrections to deflection angles, potentially offering distinctive observational signatures of modified gravity effects [33]. Our analysis incorporates these plasma effects through an optical metric approach, revealing how the interaction between the KZ deformation parameter η and the plasma frequency alters lensing observables across different wavelengths.

BH thermodynamics constitutes another fundamental domain in which modified gravity effects induce significant alterations in classical predictions [34–36]. The pioneering work of Bekenstein and Hawking established the connection between the BH event horizon area and entropy, along with the identification of surface gravity with temperature [37]. These relationships form the foundation of BH thermodynamics, providing a crucial bridge between gravitational physics and quantum theory [38–41]. For SKZ BHs, the deformation parameter η introduces significant modifications to the horizon structure, Hawking temperature profile, and overall thermodynamic behavior. These modifications potentially influence critical phenomena such as BH phase transitions, evaporation dynamics, and ultimate fate. Incorporation of quantum corrections to the BH entropy represents an essential refinement to the thermodynamic framework. Various approaches, including string theory, loop quantum gravity, and effective field theory, suggest corrections to the standard Bekenstein-Hawking area law. The exponential correction entropy formalism, which we employ in our analysis, introduces quantum modifications through a correction term proportional to e^{-S_0}, where S_0 represents the classical entropy [42, 43]. This approach captures leading-order quantum effects while maintaining analytical tractability, allowing for systematic investigation of how quantum corrections influence thermodynamic quantities such as internal energy, Helmholtz free energy, and heat capacity.

Our primary motivation for investigating static SKZ BHs stems from their unique position at the intersection of theoretical gravity, quantum physics, and observational astrophysics. By examining both gravitational lensing and thermodynamic properties within a unified framework, we aim to establish comprehensive signatures that could potentially distinguish these modified spacetimes from their classical counterparts. The deformation parameter η serves as a quantitative measure of deviation from GR, potentially encapsulating effects from quantum gravity, higher-curvature corrections, or exotic matter fields. Through systematic analysis of how this parameter influences observable phenomena, we seek to establish observational constraints and theoretical insights into physics beyond the standard BH paradigm.

The present investigation aims to achieve several specific objectives: (1) derive analytical expressions for deflection angles of light and massive particles in SKZ spacetime using complementary methodological approaches; (2) characterize magnification properties and critical curve structures induced by the deformation parameter; (3) analyze plasma-induced corrections to gravitational lensing in modified gravity backgrounds; (4) examine thermodynamic behavior with particular focus on quantum-corrected entropy formulations; and (5) establish constraints on the deformation parameter η based on theoretical consistency requirements and observational implications. Through this comprehensive analysis, we seek to improve the understanding of the effects of modified gravity on BH physics while establishing a theoretical foundation for future observational tests using next-generation astronomical facilities.

The paper is organized as follows: Section II provides a comprehensive review of the SKZ BH geometry, establishing the mathematical foundation for subsequent analyses. Section III develops a perturbative formulation for gravitational lensing in SKZ spacetime, deriving analytical expressions for deflection angles through classical geodesic approaches. Section IV extends this analysis to magnification properties, characterizing how image distortions and brightness amplifications are modified by the deformation parameter. Section V employs the GB theorem to compute topological corrections to gravitational lensing, offering an alternative perspective on deflection phenomena. Section VI incorporates plasma effects into the lensing formalism, revealing frequency-dependent signatures in deflection angles. Section VII

investigates the behavior of massive particles in SKZ geometry through the Jacobi metric approach, demonstrating velocity-dependent corrections to gravitational deflection. Section VIII examines thermodynamic properties with emphasis on quantum-corrected entropy formulations, analyzing stability conditions and phase structures. Finally, Section IX synthesizes our findings, discusses their astrophysical implications, and outlines directions for future research.

II. SKZ BH GEOMETRY

This section presents a comprehensive formulation of the SKZ BH geometry, establishing the mathematical foundation upon which subsequent analyses of thermodynamic properties and gravitational lensing phenomena are constructed. Following the framework initially developed by Konoplya and Zhidenko [7], we systematically implement parametric deformations to the standard Schwarzschild solution while preserving asymptotic flatness.

We begin with the standard Schwarzschild BH line element characterized by mass M:

$$ds_s^2 = f_s(r)dt^2 - \frac{1}{f_s(r)}dr^2 - r^2 d\Omega^2, \tag{1}$$

where $f_s(r) \equiv 1-2M/r$ and $d\Omega^2 \equiv d\theta^2+\sin^2\theta d\varphi^2$ represents the line element of a unit sphere. The fundamental innovation of the KZ approach [44] lies in the introduction of parametric deformations to the mass term through a power series expansion:

$$M \to M + \frac{1}{2}\sum_{i=0}^{\infty}\frac{\eta_i}{r^i}, \tag{2}$$

which consequently modifies the metric function $f_s(r)$ as:

$$f_s(r) \to 1 - \frac{2M}{r} - \sum_{i=0}^{\infty}\frac{\eta_i}{r^{i+1}}. \tag{3}$$

To maintain consistency with the asymptotic behavior of the Schwarzschild solution at large distances, we impose the constraint $\eta_0 = 0$. Furthermore, experimental constraints from the parameterized post-Newtonian formalism [45] derived from Cassini data [46] and Lunar Laser Ranging measurements [47] establish:

$$\frac{\eta_1}{2} \leqslant 2.3 \times 10^{-4}. \tag{4}$$

Based on these theoretical and observational constraints, we set $\eta_1 = 0$ and focus our analysis on a single deformation parameter in the mass term:

$$M \to M + \frac{\eta}{2\,r^2}, \tag{5}$$

where η represents the KZ deformation parameter, mathematically equivalent to setting $\eta_i = \eta\,\delta_{i\,2}$ in the general expansion. This formulation yields the line element of the Static KZ BH [9]:

$$ds^2 = \left(1 - \frac{2M}{r} - \frac{\eta}{r^3}\right)dt^2 - \left(1 - \frac{2M}{r} - \frac{\eta}{r^3}\right)^{-1} dr^2 - r^2 d\Omega^2, \tag{6}$$

with the corresponding metric function:

$$f_{KZ}(r) \equiv 1 - \frac{2M}{r} - \frac{\eta}{r^3}. \tag{7}$$

The event horizon, defined by the condition $f_{KZ}(r) = 0$, is determined by solving a cubic equation that yields three potential solutions $r_i(\eta)$. A straightforward analysis demonstrates that $r_2(\eta)$ never constitutes a physical horizon [9]. For the remaining solutions $r_1(\eta)$ and $r_3(\eta)$, there exists a critical threshold $\eta_{\min} = -32/27M^3$ below which the SKZ spacetime would manifest as a naked singularity, violating the cosmic-censorship conjecture.

For parameter values within the range $-32/27M^3 \leq \eta < 0$, both $r_1(\eta)$ and $r_3(\eta)$ represent physical horizons, with $r_1(\eta)$ functioning as the event horizon. In contrast, for positive values of η, only $r_1(\eta)$ constitutes a physical horizon. Throughout our subsequent analysis, we denote the event horizon radius as $r_h(\eta) \equiv r_1(\eta)$ and restrict our investigation to the parameter domain $\eta \geq \eta_{\min}$.

The explicit mathematical expressions for the three solutions to the horizon equation are:

$$r_1(\eta) = \frac{1}{3}\left(2M + \frac{4\sqrt[3]{2}M^2}{A(\eta)} + \frac{A(\eta)}{\sqrt[3]{2}}\right), \tag{8}$$

$$r_2(\eta) = \frac{1}{3}\left(2M - \frac{2\sqrt[3]{2}(1+i\sqrt{3})M^2}{A(\eta)} - \frac{(1-i\sqrt{3})A(\eta)}{2\sqrt[3]{2}}\right), \tag{9}$$

$$r_3(\eta) = \frac{1}{3}\left(2M - \frac{2\sqrt[3]{2}(1-i\sqrt{3})M^2}{A(\eta)} - \frac{(1+i\sqrt{3})A(\eta)}{2\sqrt[3]{2}}\right), \tag{10}$$

where

$$A(\eta) \equiv \sqrt[3]{16M^3 + 27\eta + 3\sqrt{3}\sqrt{32M^3\eta + 27\eta^2}}. \tag{11}$$

The KZ deformation parameter η exerts significant influence on the event horizon location, enabling SKZ BHs with identical ADM mass M to manifest different horizon radii. The event horizon area, given by $A(\eta) = 4\pi r_h^2(\eta)$, increases systematically with increasing deformation parameter η.

It is crucial to emphasize that the SKZ metric does not represent a solution to Einstein's field equations but rather constitutes a parametric deviation from the Schwarzschild geometry that preserves asymptotic flatness while introducing controlled modifications to the near-horizon region. This approach enables systematic

investigation of potential deviations from GR without commitment to specific alternative gravitational theories [48].

The computation of Hawking temperature for the SKZ BH proceeds from the surface gravity formulation:

$$T_H = \frac{f'_{KZ}(r_h)}{4\pi} \tag{12}$$

Evaluating this expression at the event horizon yields:

$$T_H = \frac{M}{2\pi r_h^2} + \frac{3\eta}{4\pi r_h^4} \tag{13}$$

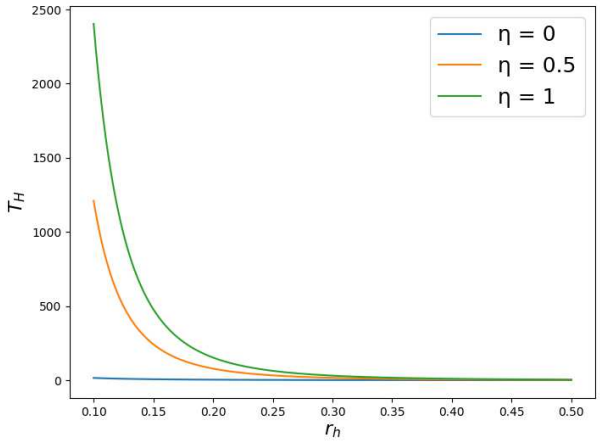

FIG. 1: Variation of Hawking temperature with respect to event horizon radius (r_h) for different values of the deformation parameter η, with mass parameter fixed at $M = 1$. The plot demonstrates that positive deformation parameters significantly enhance thermal radiation for small BHs, introducing temperature profiles that deviate markedly from the classical Schwarzschild behavior.

Figure 1 illustrates the functional dependence of Hawking temperature T_H on the radius of the event horizon r_h at different values of the deformation parameter η. For the classical Schwarzschild BH ($\eta = 0$, blue curve), the temperature exhibits an inverse proportionality relationship with horizon radius, manifesting elevated temperatures for microscopic BHs. However, as the deformation parameter increases ($\eta = 0.5, 1$), the temperature profiles undergo significant modification, exhibiting more rapid growth at small horizon radii compared to the classical case. This behavior reveals the profound thermodynamic implications of the deformation parameter, suggesting that quantum gravity or modified gravity effects potentially become increasingly significant below certain critical length scales. The enhanced temperature gradients for positive values η indicate that geometric deformations potentially accelerate the evaporation process by intensifying radiative emissions, particularly for small BHs where geometry modifications near the horizon exert their strongest influence.

III. PERTURBATIVE ANALYSIS OF GRAVITATIONAL LENSING IN SKZ BH SPACETIME: CLASSICAL APPROACH

In this section, we develop a perturbative formulation for analyzing the trajectories of test particles within the gravitational field of a SKZ BH. Our primary objective is to derive a second-order differential equation for the inverse radial coordinate, defined as $u = 1/r$, as a function of the azimuthal angle φ. This methodological approach extends previous investigations by Briet and Hobill [49] (and recently by Sucu and Sakallı [43]) on null geodesics, while specifically focusing on determining the light deflection angle in the presence of the KZ parametric deformation.

The equations of motion governing this system can be derived either by varying the Lagrangian associated with massless particles or directly from the null geodesic equations [50]. Given the inherent spherical symmetry of the metric (6) and considering planar motion at $\theta = \pi/2$, we can simplify our analysis by neglecting variations in the polar angle. Consequently, the equations of motion are expressed as:

$$E \equiv f_{KZ}\frac{dt}{d\lambda}, \tag{14}$$

$$\mathcal{J} \equiv r^2\frac{d\varphi}{d\lambda}, \tag{15}$$

$$0 = \frac{d}{d\lambda}\left(2f_{KZ}^{-1}\frac{dr}{d\lambda}\right) + (f_{KZ})'\left(\frac{dt}{d\lambda}\right)^2 - (f_{KZ}^{-1})'\left(\frac{dr}{d\lambda}\right)^2 - 2r\left(\frac{d\varphi}{d\lambda}\right)^2. \tag{16}$$

In this formulation, the quantities E and $\mathcal{J}$ represent conserved constants corresponding to the photon's energy and angular momentum, respectively. The geodesic path is parameterized by an affine parameter λ, with the prime symbol denoting differentiation with respect to r. The impact parameter, a critical element in gravitational lensing studies [43], is defined as $b = \frac{\mathcal{J}}{E}$.

Through substitution of Eqs. (14) and (15) into Eq. (16) and introducing the transformation $u = 1/r$, while redefining φ as the independent variable, we derive a second-order differential equation for the inverse radial distance u:

$$\frac{d^2u}{d\varphi^2} + f_{KZ}u = -\frac{1}{2}u^2\frac{d}{du}\left(f_{KZ}\right), \tag{17}$$

This formulation, when developed using the specific form of f_{KZ} for the SKZ BH, yields the following differential equation:

$$\frac{d^2u}{d\varphi^2} + u = 3Mu^2 + \frac{5}{2}\eta u^4. \tag{18}$$

The structure of Eq. (18) reveals how the deformation parameter η introduces higher-order perturbations to the standard Schwarzschild lensing equation, manifesting as a u^4 term that significantly modifies light propagation in strong gravitational fields.

To solve this equation analytically, we employ a perturbative approach by expanding the solution in a power series:

$$u = u_0 + \varepsilon u_1 + \varepsilon^2 u_2 + \cdots, \tag{19}$$

This expansion allows us to approximate the solution to any desired order in the small parameter ε, which physically corresponds to the strength of gravitational interaction. For the zeroth-order or homogeneous equation:

$$\frac{d^2u_0}{d\varphi^2} + u_0 = 0, \tag{20}$$

The solution is $u_0 = \mho\cos\varphi$, where $\mho$ represents the inverse impact parameter ($\mho = 1/b$), corresponding at this level to the reciprocal of the closest approach distance in the unperturbed trajectory. Following this zeroth-order approximation, the equations for higher-order corrections are systematically derived:

$$\frac{d^2u_1}{d\varphi^2} + u_1 = 3\mho\cos^2\varphi, \tag{21}$$

$$\frac{d^2u_2}{d\varphi^2} + u_2 = 6\cos\varphi u_1 + \frac{5}{2}\frac{\eta\mho^2\cos\varphi^4}{M^2}, \tag{22}$$

These differential equations admit analytical solutions, yielding the first-order and second-order corrections:

$$u_1 = \frac{\mho\left(3 - \cos(2\varphi)\right)}{2}, \tag{23}$$

$$u_2 = \frac{\mho}{48M^2}\Big(9M^2\cos(3\varphi) - 8\mho\left(\cos^4(\varphi) + 4\cos^2(\varphi) - 8\right)\eta + 180\sin(\varphi)\varphi M^2\Big). \tag{24}$$

Combining these results according to Eq. (19), we obtain a comprehensive perturbative solution for the trajectory:

$$\frac{u}{\mho} \simeq \cos\varphi + \frac{1}{2}\mho\big(3 - \cos(2\varphi)\big)M + \frac{\mho^2}{48}\Big(9M^2\cos(3\varphi) - 8\mho\left(\cos^4(\varphi) + 4\cos^2(\varphi) - 8\right)\eta + 180\sin(\varphi)\varphi M^2\Big). \tag{25}$$

For determining the light deflection angle α_{def} at asymptotically large distances, we exploit the symmetry properties of the trajectory about $\varphi = 0$. By introducing the coordinate transformation:

$$\varphi = \frac{\pi}{2} + \psi, \tag{26}$$

where ψ represents a small angular deviation, the total deflection angle is given by:

$$\alpha_{def} = 2\psi. \tag{27}$$

Expanding this result to second order in the small parameter $\varepsilon = M\mho = M/b$, we derive the analytical expression for the deflection angle:

$$\alpha_{def} \approx \frac{4M}{b} + \frac{15M^2\pi}{4b^2} + \frac{8\eta}{3b^3}. \tag{28}$$

This expression explicitly demonstrates how the deformation parameter η introduces a contribution proportional to b^{-3}, a novel feature not present in the standard Schwarzschild lensing. Recent observational advancements in gravitational lensing potentially offer empirical constraints on this parameter.

To reformulate our findings in terms of the distance of closest approach r_0, we recognize that the zeroth-order approximation $\mho$ corresponds to $1/r_{min}$. More precisely, at the perihelion point where $\varphi = 0$, the following relation holds:

$$\frac{1}{r_{min}} = \mho + \mho^2 M + \frac{3}{16}\mho^3 M^2 + \frac{1}{2}\mho^4\eta. \tag{29}$$

Substituting this relation into our expression for the deflection angle, we obtain an expansion in powers of $1/r_{min}$:

$$\alpha_{def} \approx \frac{4M}{r_{min}} + \frac{\left(-16 + 15\pi\right)M^2}{4r_{min}^2} - \frac{45M^3\pi - 16\eta}{6r_{min}^3}. \tag{30}$$

This reformulation provides important physical insights, as r_{min} represents the actual minimal distance of approach in the gravitational field, a quantity more directly related to observational phenomena than the impact parameter b defined at asymptotic infinity. The contribution of the deformation parameter η appears in the third-order term, suggesting that its effects become particularly significant for light rays passing close to the BH, where higher-order terms in the deflection angle expansion gain importance. Fig. 2 illustrates both the observational manifestation and theoretical framework of gravitational lensing in the context of SKZ BHs. The visualization in panel (a) demonstrates how light rays from background sources undergo significant deflection when

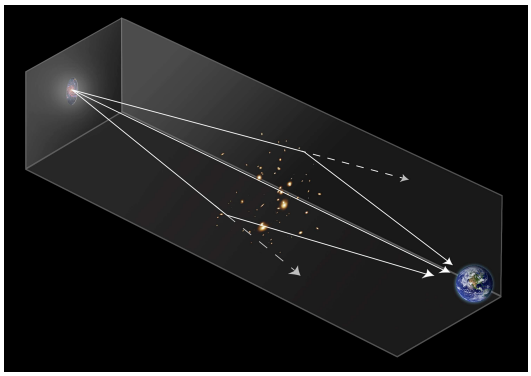

(a)

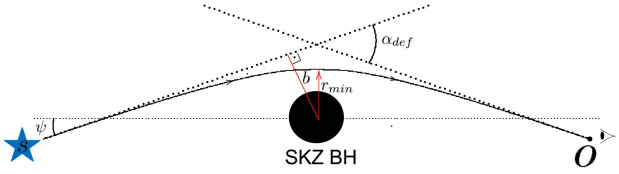

(b)

FIG. 2: (a) Gravitational lensing visualization depicting how light from distant galaxies is distorted by an intervening massive object, creating multiple images and extended arcs. This phenomenon emerges directly from the spacetime curvature described by the deflection angle in Eq. (30) (Credit: NASA, ESA, Ann Feild (STScI), Frank Summers (STScI) [51]). (b) Schematic representation of the SKZ BH lensing geometry, illustrating the deflection angle α_{def}, impact parameter b, and the angular separations between source, observer, and resulting images.

traversing the vicinity of massive objects, resulting in characteristic distortion patterns that serve as observational signatures of spacetime curvature. Panel (b) provides a schematic representation of the lensing geometry specific to SKZ BHs, where the incorporation of the deformation parameter η introduces additional complexity to the deflection phenomena, particularly through third-order contributions to α_{def} as analytically expressed in Eq. (30). This modification becomes increasingly significant for light rays passing in close proximity to the BH, potentially offering an observational mechanism for constraining deviations from standard Schwarzschild geometry.

IV. MAGNIFICATION PROPERTIES OF SKZ BHS

The gravitational lensing phenomenon, particularly the magnification effects induced by SKZ BHs, provides crucial insights into the spacetime deformation characterized by the parameter η. This section systematically analyzes how the magnification properties are modified by the KZ deformation parameter, extending beyond conventional Schwarzschild lensing models [52, 53].

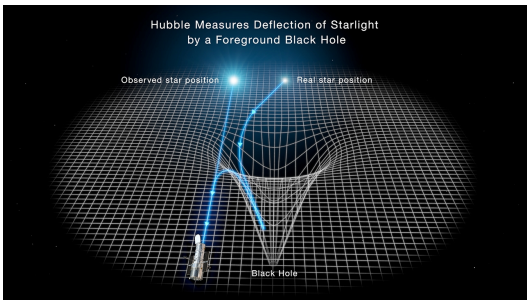

(a)

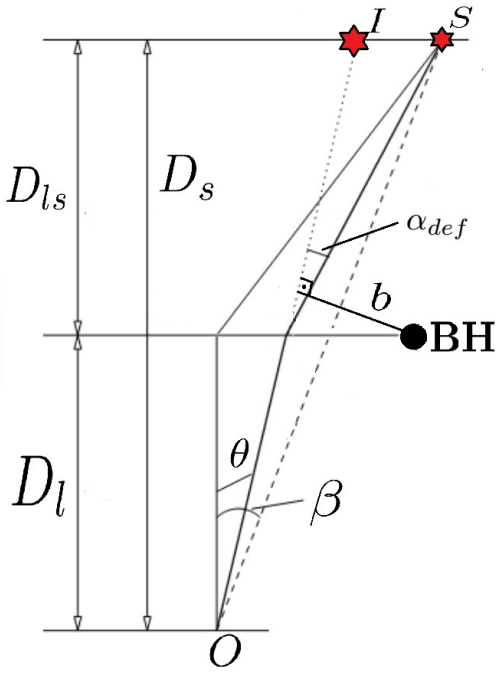

(b)

FIG. 3: (a) Hubble's observations illustrate how the gravity of a foreground BH bends and deflects the light from a distant star (Credit: Hubblesite.org [54]). (b) Lensing illustration of a BH: O is the observer, S is the source, BH is the BH acting as a gravitational lens, I is the position of the image. β is the angle between the source and the optical axis, θ is the angle between the image and the optical axis, $\alpha_{\rm def}$ is the deflection angle. b is the impact parameter and D_l, D_s and D_{ls} are angular diameter distances (from observer to lens, from observer to source, and from lens to source, respectively). The dashed line represents the path light would take in the absence of the lens, while the solid line shows the actual path of light due to gravitational lensing.

Fig. 3 illustrates the fundamental lensing geometry for SKZ BHs. Through this geometric configuration and the deflection angle formalism established in Eq. (28), we can determine the mathematical relationship between source

and image positions. The spherical symmetry of the SKZ metric ensures that only radial distances are affected by lensing, while the azimuthal angle φ remains invariant. This geometric constraint leads to the following relationship [55]:

$$(\beta - \theta)D_{\rm s} = \alpha_{\rm def} D_{\rm ls} \tag{31}$$

This equation can be reformulated as:

$$\beta = \theta + \frac{D_{\rm ls}}{D_{\rm s}}\alpha_{\rm def}\ . \tag{32}$$

It is imperative to note that in this section, we employ SI units rather than natural units for improved observational applicability. This necessitates the explicit inclusion of gravitational constant G and speed of light c in our formulations. Specifically, the mass parameter M and the deformation parameter η have been transformed according to $M \to M \cdot G/c^2$ and $\eta \to \eta \cdot G^3/c^6$, respectively. This transformation enables direct comparison with observational data from astronomical surveys. Incorporating our previously derived deflection angle from Eq. (28), the lens equation for the SKZ BH becomes:

$$\beta = \theta + \frac{\tilde{\theta}^2_{\rm Ein}}{\theta}, \tag{33}$$

in which

$$\tilde{\theta}^2_{\rm Ein} = \theta^2_{\rm Ein}\left(1 + \frac{15\pi GM}{16\theta c^2 D_l} + \frac{2G^2\eta}{3M\theta^2 c^4 D_l^2}\right), \tag{34}$$

in which $\theta_{\rm Ein}$ denotes the well-known Einstein angle, which is given by

$$\theta^2_{\rm E} = \frac{4GM}{c^2}\frac{D_{\rm ls}}{D_{\rm s}D_1}. \tag{35}$$

Recent theoretical developments by Ghosh et al. [56] have demonstrated that gravitational lensing affects not only the directional properties of light but also modifies the cross-sectional area of ray bundles. This cross-sectional modification directly influences the observed brightness of lensed objects, a phenomenon quantified through magnification calculations. For an infinitesimally small source, the magnification factor μ is given by [55]:

$$\mu^{-1} = \left|\frac{\beta}{\theta}\frac{d\beta}{d\theta}\right|\ . \tag{36}$$

This formulation reveals that the image undergoes magnification or demagnification by a factor $|\mu|$. In situations where multiple images are formed from a single source, the total amplification is calculated as the sum of individual image magnifications, as demonstrated by Virbhadra and Ellis [57].

From the lens equation, we can derive expressions for the tangential and radial critical curves, which represent loci of theoretically infinite magnification:

$$\mu_{\rm tan} = \left|\frac{\beta}{\theta}\right|^{-1} = \theta^2\left(\theta^2 + \tilde{\theta}^2_{\rm Ein}\right)^{-1}, \tag{37}$$

and

$$\mu_{\rm rad} = \left|\frac{d\beta}{d\theta}\right|^{-1} = \theta^2\left(\theta^2 - \tilde{\theta}^2_{\rm Ein}\right)^{-1}. \tag{38}$$

A distinctive characteristic emerges in the analysis of these magnification components: $\mu_{\rm rad}$ exhibits a singularity at $\theta = \theta_{\rm E}$, which corresponds to the angular radius of the radial critical curve. Conversely, $\mu_{\rm tan}$ maintains finite values throughout the parameter space. This differential behavior indicates that the SKZ BH produces specific lensing signatures that could potentially be observationally distinguished from other compact object models.

Fig. 4 presents a comprehensive visualization of magnification curves—tangential, radial, and total—for three distinct BH configurations. Panel (a) illustrates the standard Schwarzschild case ($\eta = 0$), serving as our reference model. Panels (b) and (c) depict SKZ BHs with progressively increasing deformation parameters: $\eta = 1 \times 10^{19} M_\odot^3$ and $\eta = 1 \times 10^{20} M_\odot^3$, respectively. These numerical values are consistent with the theoretical constraints established by Konoplya and Zhidenko [7] and fall within observational bounds derived from Event Horizon Telescope data.

The comparative analysis of these magnification profiles reveals significant structural differences contingent upon the value of η. In the Schwarzschild limit (panel a), the magnification behavior follows established patterns documented in classical lensing theory. However, as η increases (panels b and c), we observe systematic modifications in both the position and amplitude of magnification peaks, particularly in the radial component $\mu_{\rm rad}$. Of particular interest is the emergence of enhanced radial magnification at specific angular distances as η increases. This phenomenon suggests that SKZ BHs with substantial deformation parameters could produce distinctive observational signatures in microlensing light curves. Such signatures, if detected, would provide empirical constraints on the deformation parameter η and, by extension, offer insights into potential modifications of general relativity in strong gravitational regimes. The tangential magnification component $\mu_{\rm tan}$ exhibits more subtle variations with changing η, indicating that tangential arcs—common in galaxy cluster lensing—may not serve as optimal observational targets for discriminating between Schwarzschild and SKZ BHs. Instead, radial magnification features, particularly the position and profile of radial critical curves, emerge as more promising

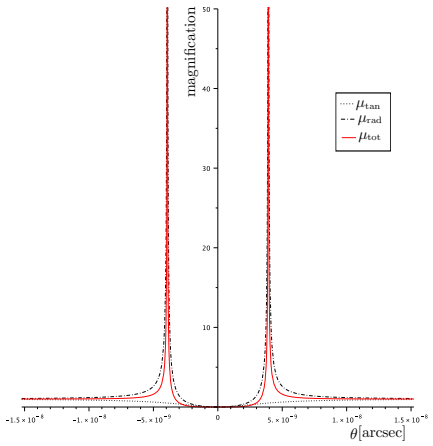

(a)

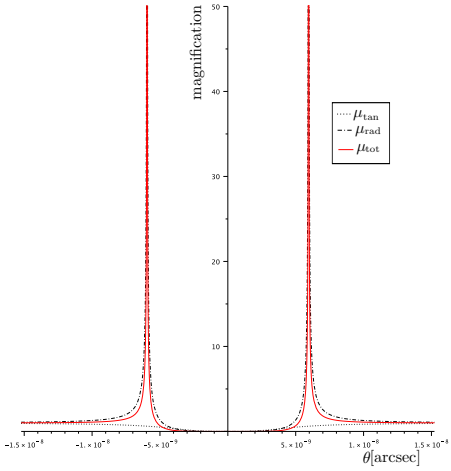

(b)

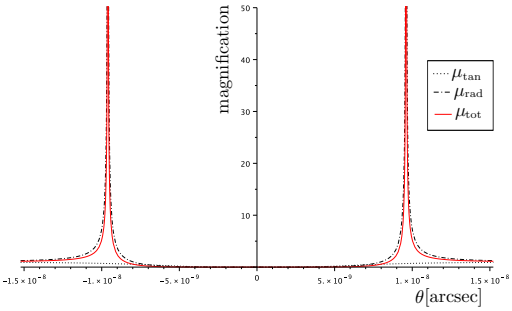

(c)

FIG. 4: The magnifications: tangential $\mu_{\rm tan}$ (dotted lines), radial $\mu_{\rm rad}$ (dash-dotted lines), and total μ (continuous curves), are plotted as functions of the image position θ for three BH cases; (a) is for the Schwarzschild BH ($\eta = 0$), (b) panel represents the SKZ BH with $\eta = 1 \times 10^{18} M_\odot^3$, and (c) panel stands for $\eta = 1 \times 10^{19} M_\odot^3$. The singularities of $\mu_{\rm tan}$ and $\mu_{\rm rad}$ give the positions of the tangential and radial critical curves, respectively. In the upper panel the singularity is in the tangential critical curve, in the bottom panel, instead, in the radial critical curve. Here $|M| = 1\, M_\odot$, $D_{\rm s} = 0.05$ Mpc and $D_{\rm l} = 0.01$ Mpc. Angles are given in arcseconds: 1 arcsec $= 4.848 \times 10^{-6}$ rad.

diagnostics for detecting spacetime deformations characterized by the KZ metric. We believe that these theoretical predictions establish a framework for future observational tests using high-resolution instruments such as the James Webb Space Telescope and next-generation very long baseline interferometry arrays [58, 59].

V. TOPOLOGICAL CORRECTIONS TO GRAVITATIONAL LENSING OF SKZ BH

In this section, we implement a topological approach to compute weak deflection angles in the SKZ BH geometry, providing complementary insights to the perturbative analysis presented in Section III. The GB theorem offers a particularly elegant framework for investigating gravitational lensing phenomena from a global topological perspective rather than through local geodesic properties [52]. This approach not only yields computationally efficient derivations but also elucidates the fundamental geometric nature of light deflection in curved spacetimes [60].

Our analysis begins with null geodesics that satisfy the condition $ds^2 = 0$. By implementing the coordinate transformation $dr^* = \frac{1}{A} dr$, we reformulate the optical metric into the following form:

$$dt^2 = dr^{*2} + \tilde{f}^2(r^*) d\varphi^2, \tag{39}$$

where $\tilde{f}(r^*) = r\sqrt{\frac{1}{f(r)}}$, with the equatorial plane defined by $\theta = \pi/2$. This reformulation facilitates the application of the GB theorem to the optical geometry.

The Gaussian curvature, a fundamental quantity in this approach, is calculated as:

$$\mathcal{K} = \frac{R_{r\varphi r\varphi}}{\gamma} = \frac{1}{\sqrt{\gamma}} \left[\frac{\partial}{\partial \varphi} \left(\frac{\sqrt{\gamma}}{\gamma_{rr}} \Gamma^{\varphi}_{rr} \right) - \frac{\partial}{\partial r} \left(\frac{\sqrt{\gamma}}{\gamma_{rr}} \Gamma^{\varphi}_{r\varphi} \right) \right]. \tag{40}$$

For the SKZ BH geometry, this calculation yields:

$$\mathcal{K} \approx \frac{3M^2}{r^4} - \frac{2M}{r^3} + \frac{11M\eta}{r^6} - \frac{6\eta}{r^5} + \frac{15\eta^2}{4r^8}. \tag{41}$$

The presence of the deformation parameter η introduces additional curvature terms that modify the deflection properties compared to the standard Schwarzschild case, particularly at higher orders in $1/r$.

To systematically apply the GB theorem, we consider a compact, oriented, non-singular domain D with Euler characteristic $\chi(D)$, bounded by a piecewise smooth curve with geodesic curvature κ. The theorem states:

$$\int\int_D \mathcal{K} dS + \oint_{\partial D} \kappa dt + \sum_{i=1} \beta_i = 2\pi\chi(D). \tag{42}$$

For our analysis, we construct an integration domain $\tilde{D}$ enclosed by a geodesic connecting the source S and observer O, together with a circular arc C_R that intersects the geodesic at right angles. This construction simplifies the theorem to:

$$\int\int_{\tilde{D}} \mathcal{K}dS + \int_{C_R} \kappa dt = \pi. \tag{43}$$

The geodesic curvature of C_R is calculated as:

$$\kappa(C_R) = \left(\nabla_{\dot{C}_R}\dot{C}_R\right)^r = \dot{C}_R^{\varphi}(\partial_\varphi \dot{C}_R^r) + \Gamma^r_{\varphi\varphi}(\dot{C}_R^{\varphi})^2, \tag{44}$$

where $\Gamma^r_{\varphi\varphi} = -\tilde{f}(r^*)\tilde{f}'(r^*)$ and $(\dot{C}_R^{\varphi})^2 = \frac{1}{\tilde{f}^2(r^*)}$. Taking the limit as $R \to \infty$, we obtain:

$$\lim_{R\to\infty}[\kappa(C_R)dt] = \lim_{R\to\infty}[-\tilde{f}'(r^*)]d\varphi = d\varphi. \tag{45}$$

Incorporating this result into the GB theorem leads to:

$$\int\int_{\tilde{D}_{R\to\infty}} \mathcal{K}dS + \int_0^{\pi+\alpha} d\varphi = \pi. \tag{46}$$

The surface element in the equatorial plane is expressed as:

$$dS = \sqrt{\gamma}drd\varphi = \frac{r}{f^{3/2}(r)}drd\varphi. \tag{47}$$

This formulation allows us to determine the deflection angle through:

$$\begin{aligned}\alpha &= -\int_0^{\pi}\int_{\frac{b}{\sin\varphi}}^{\infty} \mathcal{K}dS \\ &\simeq \frac{8\eta}{3b^3} + \frac{4M}{b} + \frac{3M^2\pi}{4b^2} - \frac{4M^3}{b^3} + \mathcal{O}\left(\left(\frac{M}{b}\right)^4\right)\end{aligned} \tag{48}$$

In this expression, we employ the weak deflection approximation using the zeroth-order trajectory $r = b/\sin\varphi$ within the integration interval $0 \le \varphi \le \pi$. The deformation parameter η introduces additional terms in the deflection angle, most notably the contributions proportional to b^{-3} and b^{-4}, which represent distinctive signatures of the modified geometry.

Figure 5 illustrates the dependence of the deflection angle α on the impact parameter b for various values of the deformation parameter η. The results demonstrate a pronounced enhancement of deflection for increasing values of η, particularly at small impact parameters where the gravitational field is strongest. This behavior underscores the potential observational significance of the deformation parameter in strong-field lensing scenarios, where light rays pass in close proximity to the BH.

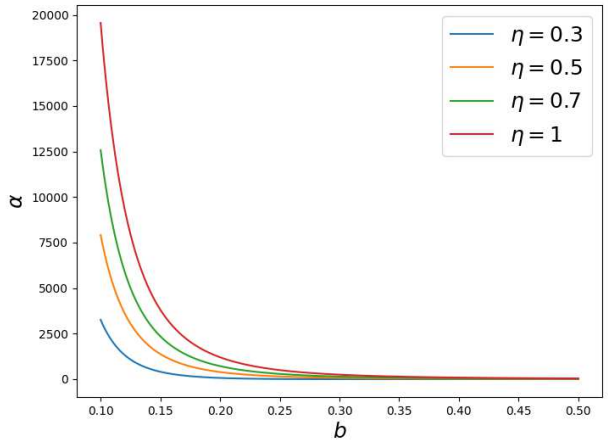

FIG. 5: The difference of the deflection angle α for varying values of η, with fixed $M = 1$, in relation to the impact parameter b. The findings indicate an enhanced gravitational lensing effect in areas of significant curvature, with larger η values producing a greater deflection, particularly for small b. The impact of η becomes less important as the deflection angle quickly decreases for increasing b.

The topological approach implemented here offers several advantages over conventional geodesic calculations. First, it provides a global perspective on deflection phenomena, emphasizing the integral geometric character of light bending in curved spacetimes. Second, it establishes a direct connection between the Gaussian curvature of the optical metric and the resulting deflection angle, thereby illuminating the fundamental geometric principles underlying gravitational lensing. Finally, this method facilitates straightforward computational extensions to more complex scenarios, including plasma media and alternative gravity theories.

The leading orders of the deflection angle derived through the GB approach exhibits excellent agreement with the perturbative results obtained in Sec. III, validating the consistency of our analysis. The topological formulation, however, offers additional conceptual insights regarding the global geometric underpinnings of gravitational lensing phenomena in deformed BH spacetimes.

VI. PLASMA-INDUCED CORRECTIONS TO GRAVITATIONAL LENSING NEAR SKZ BH

The propagation of electromagnetic radiation through astrophysical plasma environments in curved spacetime represents a critical frontier in gravitational lensing theory, with significant observational implications [61]. Unlike vacuum propagation, plasma introduces frequency-dependent refractive effects that couple with the under-

lying gravitational field, yielding distinctive chromatic signatures in lensing phenomena. This section systematically analyzes how plasma modifies gravitational deflection angles in the vicinity of SKZ BHs, extending our previous topological approach to incorporate these frequency-dependent effects.

We begin by formulating the refractive index $n(r)$ which encapsulates both the plasma properties and gravitational redshift effects [24, 62, 63]:

$$n(r) = \sqrt{1 - \frac{\omega_p^2(r)}{\omega_0^2(r)} f(r)}, \tag{49}$$

where ω_p represents the plasma frequency of electrons, and ω_0 denotes the photon frequency observed at asymptotic infinity. This formulation accounts for the interaction between plasma dispersion and spacetime curvature, yielding frequency-dependent modifications to light propagation paths.

The corresponding optical metric for photon propagation in plasma-filled SKZ spacetime takes the form:

$$dt^2 = g_{lm}^{\rm opt} dx^l dx^m = n^2 \left(\frac{1}{f^2(r)} dr^2 + \frac{r^2}{f(r)} d\varphi^2 \right), \tag{50}$$

where $f(r)$ is defined according to the SKZ metric introduced in Sec. II. This optical metric characterizes the effective geometry experienced by photons traversing the plasma medium around the deformed BH.

The Gaussian optical curvature $\tilde{\mathcal{K}}$, which governs deflection properties in this medium, is determined from the Ricci scalar R as:

$$\tilde{\mathcal{K}} = \frac{\mathcal{R}_{r\varphi r\varphi}(g^{opt})}{\det g^{opt}}, \tag{51}$$

with the determinant of the optical metric given by:

$$\det(g^{opt}) = \frac{n(r)^4 r^2}{f(r)^3}. \tag{52}$$

Through systematic calculation, we obtain the following approximation for the Gaussian optical curvature in the SKZ geometry:

$$\begin{aligned}\tilde{\mathcal{K}} \approx & -\frac{2M}{r^3} - \frac{6\eta}{r^5} + \frac{3M^2}{r^4} + \frac{11M\eta}{r^6} + \frac{15\eta^2}{4r^8} + \frac{48w_e^2 M\eta}{r^6 w_\infty^2} \\ & - \frac{54w_e^2 M^2\eta}{r^7 w_\infty^2} - \frac{45w_e^2 M\eta^2}{r^9 w_\infty^2} + \frac{12w_e^2 M^2}{r^4 w_\infty^2} - \frac{3w_e^2 M}{r^3 w_\infty^2} \\ & - \frac{21w_e^2\eta}{2r^5 w_\infty^2} + \frac{21w_e^2\eta^2}{r^8 w_\infty^2} - \frac{12w_e^2 M^3}{r^5 w_\infty^2} - \frac{21w_e^2\eta^3}{2r^{11} w_\infty^2},\end{aligned} \tag{53}$$

This expression explicitly incorporates the coupling between the deformation parameter η and plasma effects, revealing a complex interplay that modifies the effective optical geometry experienced by photons. For computational tractability, we retain terms up to second order in curvature, consistent with our previous vacuum analysis.

The differential surface element for the optical geometry is expressed as:

$$dS = \sqrt{g}\, dr\, d\varphi = \left(r - \frac{\omega_p^2}{\omega_0^2} \right) dr\, d\varphi. \tag{54}$$

Applying the GB theorem to this optical geometry, we calculate the plasma-modified deflection angle through:

$$\tilde{\alpha} = -\int_0^{\pi} \int_{\frac{b}{\sin\varphi}}^{\infty} \tilde{\mathcal{K}}\, dS. \tag{55}$$

For the SKZ BH in a plasma medium, this integration yields:

$$\begin{aligned}\tilde{\alpha} = & -\int_0^{\pi} \int_{\frac{b}{\sin\varphi}}^{\infty} \tilde{\mathcal{K}} dS \\ & \simeq \frac{27M^4\pi\sigma}{8b^4} - \frac{3M^2\pi\sigma}{4b^2} + \frac{3M^2\pi}{4b^2} - \frac{32M^3\sigma}{3b^3} - \frac{4M^3}{b^3} \\ & + \frac{6M\sigma}{b} + \frac{4M}{b} - \frac{99M\pi\eta\sigma}{64b^4} + \frac{21M\pi\eta}{32b^4} + \frac{14\eta\sigma}{3b^3} + \frac{8\eta}{3b^3} \\ & + \mathcal{O}(b^5)\end{aligned} \tag{56}$$

where $\sigma = \frac{\omega_p^2}{\omega_0^2}$ quantifies the plasma density relative to photon frequency, serving as the primary parameter that characterizes chromatic effects in gravitational lensing.

This analytical result reveals several significant features of plasma-influenced lensing in the SKZ geometry. First, it demonstrates that plasma introduces additional frequency-dependent contributions to the deflection angle, with effects scaling differently with impact parameter b compared to vacuum terms. Second, the interplay between the deformation parameter η and plasma density σ produces distinctive chromatic signatures that potentially offer observational discriminants for modified gravity effects. Third, the plasma-induced terms exhibit complex functional dependencies on mass M and deformation parameter η, highlighting the non-trivial coupling between plasma dispersion and spacetime geometry.

Figure 6 illustrates the variation of deflection angle Θ as a function of impact parameter b in a plasma medium for different values of the deformation parameter η. The results demonstrate that increasing η systematically modifies the deflection profile, with particularly pronounced effects at small impact parameters. This behavior suggests that strong-field lensing observations in plasma environments could potentially constrain deviations from standard Schwarzschild geometry.

Similarly, Figure 7 depicts the deflection angle variations with impact parameter for different plasma densi-

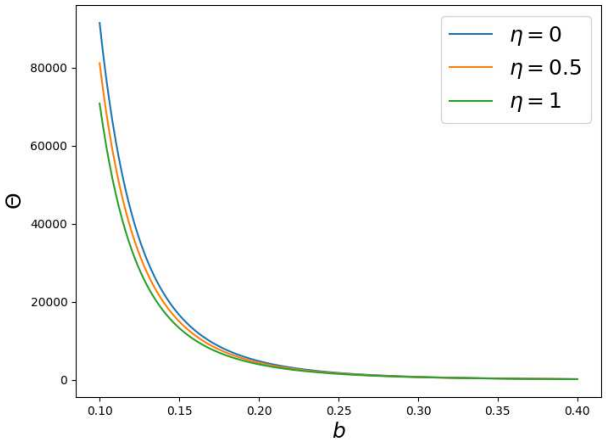

FIG. 6: The variation of the deflection angle (Θ) as a function of the impact parameter (b) in a plasma medium, considering different values of the parameter η. Here, the mass of the central object is set to $M = 1$, and the plasma parameter is taken as $\sigma = 1$. The results indicate that increasing η modifies the deflection angle, affecting the gravitational lensing behavior in a dispersive medium.

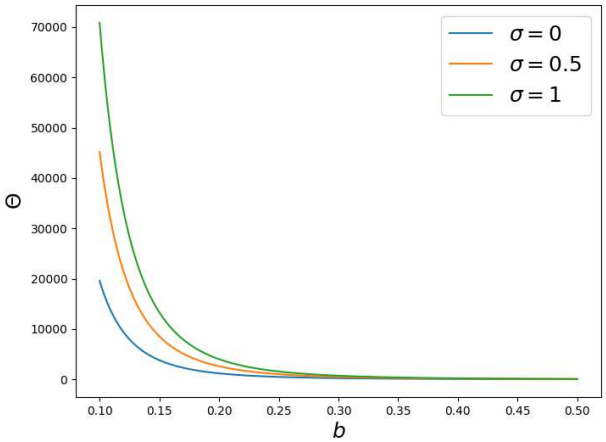

FIG. 7: The change in the deflection angle Θ in relation to the impact parameter b in a plasma medium with varying plasma parameter σ values, with $M = 1$ and $\eta = 1$ taken as constants. According to the data, the gravitational lensing effect is enhanced by increased plasma density (σ), which results in a considerable increase in the deflection angle for small b values. However, its influence decreases as b increases.

ties (characterized by σ), with fixed deformation parameter $\eta = 1$. These results reveal that higher plasma densities significantly enhance gravitational deflection, particularly at small impact parameters, while the plasma influence diminishes at larger distances from the BH.

The plasma-induced modifications to gravitational lensing have significant astrophysical implications, particularly for observations across different electromagnetic wavelengths. Radio and microwave observations, which typically traverse substantial plasma environments in galactic and intergalactic media, are especially susceptible to these chromatic effects. The frequency-dependent deflection angles predicted by our analysis suggest that multi-frequency observations of gravitationally lensed sources could potentially reveal signatures of the SKZ deformation parameter, offering novel observational probes of modified gravity theories. In the limit $\sigma \to 0$ (corresponding to high-frequency photons or low plasma density), our expression for $\tilde{\alpha}$ correctly reduces to the vacuum deflection angle derived in Sec. V, confirming the internal consistency of our formulation. This convergence demonstrates that our plasma-modified lensing framework properly encompasses the vacuum case as a limiting scenario, while systematically incorporating frequency-dependent corrections that become increasingly significant for lower-frequency observations.

VII. DEFLECTION ANGLES AND JACOBI GEOMETRY OF MASSIVE PARTICLES IN SKZ BH SPACETIME

The preceding sections have thoroughly examined null geodesics and light deflection in the SKZ BH spacetime. However, a comprehensive understanding of gravitational lensing phenomena necessitates the extension of our analysis to massive particles, whose trajectories differ fundamentally from those of photons. This section develops a rigorous mathematical framework for analyzing massive particle deflection in deformed spacetimes through the implementation of Jacobi geometry, which recasts dynamical trajectories as geodesics in an effective spatial manifold [64, 65].

The Jacobi metric approach represents a powerful theoretical formalism that unifies the treatment of massless and massive particle dynamics in curved spacetime by transforming time-dependent mechanical systems into purely geometric problems [66, 67]. This geometric reformulation offers particular advantages for investigating particle behavior in modified gravity scenarios, where standard geodesic equations may become analytically intractable. Additionally, this framework provides a natural extension to charged particles interacting with electromagnetic fields, enhancing its applicability to astrophysical contexts [68].

For a general static and spherically symmetric metric represented by equation (6), the Jacobi metric for a particle with mass m and energy E takes the form:

$$g_{ij} = (E^2 - m^2 g_{tt})\tilde{g}_{ij}, \tag{57}$$

where the optical metric is defined as:

$$\tilde{g}_{ij} = -\frac{g_{ij}}{g_{tt}}. \tag{58}$$

This construction effectively encodes the dynamics of massive particles within a modified spatial geometry, where geodesic paths correspond to physical trajectories in the original spacetime. The influence of the particle's energy-to-mass ratio manifests as a conformal factor that modifies the effective geometry experienced by the particle.

For the SKZ BH with metric function $f(r)$, the Jacobi metric simplifies to:

$$ds^2 = \left(E^2 - m^2 f(r)\right)\left[\frac{dr^2}{f^2(r)} + \frac{r^2 d\varphi^2}{f(r)}\right]. \tag{59}$$

Exploiting the spherical symmetry of the system, we restrict our analysis to the equatorial plane ($\theta = \pi/2$), where the angular momentum of the particle is conserved:

$$J = \left(E^2 - m^2 f(r)\right)\frac{r^2}{f(r)}\frac{d\varphi}{ds}. \tag{60}$$

This conservation law allows us to derive the radial equation of motion:

$$\left(\frac{dr}{ds}\right)^2 = f(r)\left(\frac{E^2}{m^2} - 1 - \frac{J^2}{m^2 r^2}\right). \tag{61}$$

By introducing the substitution $u = 1/r$, we reformulate this equation in terms of the azimuthal angle φ:

$$\left(\frac{du}{d\varphi}\right)^2 = u^4\left[\left(\frac{E}{J}\right)^2 - f(r)\left(\frac{1}{J^2} + u^2\right)\right]. \tag{62}$$

For an observer at asymptotic infinity, the energy and angular momentum of the massive particle satisfy the relativistic relations:

$$E = \frac{m}{\sqrt{1-v^2}}, \quad J = \frac{mvb}{\sqrt{1-v^2}}, \tag{63}$$

where v represents the particle's velocity at infinity and b denotes the impact parameter:

$$J = vbE. \tag{64}$$

Substituting these expressions into the Jacobi metric yields:

$$ds^2 = m^2\left(\frac{1}{1-v^2} - f(r)\right)\left[\frac{dr^2}{f^2(r)} + \frac{r^2 d\varphi^2}{f(r)}\right]. \tag{65}$$

The Gaussian curvature of this effective geometry, which determines the deflection properties of massive particles, is computed as:

$$\begin{aligned}\mathcal{K} \approx &-\frac{2M}{r^3v^6m^4} + \frac{4M}{r^3v^4m^4} - \frac{2M}{r^3v^2m^4} + \frac{16M^2}{r^4v^8m^4} \\ &- \frac{46M^2}{r^4v^6m^4} + \frac{45M^2}{r^4v^4m^4} - \frac{16M^2}{r^4v^2m^4} + \frac{M^2}{r^4m^4} - \frac{9\eta}{r^5m^4v^6} \\ &+ \frac{21\eta}{r^5m^4v^4} - \frac{15\eta}{r^5m^4v^2} + \frac{3\eta}{r^5m^4} + \mathrm{O}\left(\frac{1}{r^6}\right).\end{aligned} \tag{66}$$

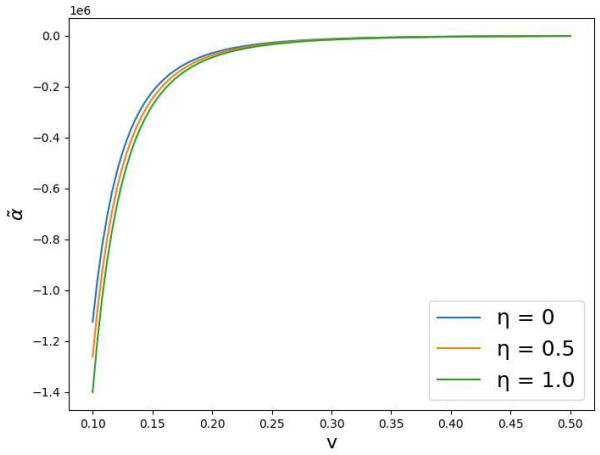

FIG. 8: Deflection angle as a function of velocity (v) for different values of parameter η, with fixed impact parameter $b = 1$ and mass $M = m = 1$. The results demonstrate that particles with lower velocities experience significantly greater deflection than those approaching the speed of light, with the deformation parameter η introducing subtle modifications to this velocity-dependent behavior.

This expression explicitly demonstrates the coupled dependence of curvature on both the deformation parameter η and particle velocity v, revealing how the effective geometry experienced by massive particles differs fundamentally from that of photons. The velocity-dependent terms introduce additional complexity to the deflection phenomena, reflecting the relativistic coupling between kinetic properties and spacetime geometry.

Applying the GB theorem to this Jacobi geometry, we derive the deflection angle for massive particles:

$$\begin{aligned}\tilde{\alpha} \approx &-\frac{M^2\pi}{4b^2m^4} - \frac{4M^3}{3b^3m^4} - \frac{27M\pi\eta}{32b^4m^4} - \frac{4\eta}{3b^3m^4} + \frac{11M^2\pi}{2b^2m^4v^2} \\ &+ \frac{64M^3}{3b^3m^4v^2} + \frac{4M}{b\,m^4v^2} + \frac{135M\pi\eta}{32b^4m^4v^2} + \frac{20\eta}{3b^3m^4v^2} - \frac{57M^2\pi}{4b^2m^4v^4} \\ &- \frac{60M^3}{b^3m^4v^4} - \frac{8M}{b\,m^4v^4} - \frac{189M\eta\pi}{32b^4m^4v^4} - \frac{28\eta}{3b^3m^4v^4} \\ &+ \mathrm{O}\left(\frac{1}{v^5}, \frac{1}{m^5}, \frac{1}{b^5}\right).\end{aligned} \tag{67}$$

This analytical result significantly extends the standard gravitational lensing formalism to encompass massive particles with arbitrary velocities, revealing the complex interplay between relativistic dynamics and modified gravity effects in the SKZ BH spacetime. The deflection angle exhibits strong velocity dependence, particularly at non-relativistic speeds, where deviations from light-like behavior become most pronounced.

Figure 8 illustrates the variation of deflection angle $\tilde{\alpha}$ with respect to particle velocity v for different values of

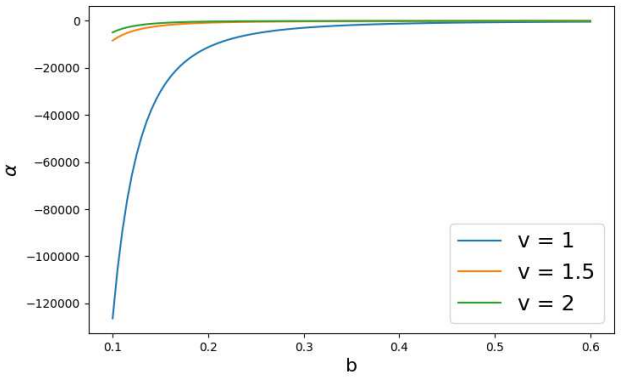

FIG. 9: Deflection angle with fixed mass $M = m = 1$ as a function of impact parameter (b) for various velocity parameter v values. With slower particles showing more sensitivity to the gravitational field at all impact parameters, the graphic shows that the impact parameter dependency of deflection changes dramatically with particle velocity.

the deformation parameter η, while maintaining fixed impact parameter $b = 1$ and mass parameters $M = m = 1$. This visualization reveals several critical features of massive particle deflection in the SKZ BH geometry. For non-relativistic velocities (small v values), the deflection angle exhibits substantial negative magnitudes, indicating significantly stronger gravitational influence compared to relativistic particles. As velocity increases toward the speed of light, the deflection angle rapidly diminishes in magnitude, asymptotically approaching the photon limit.

Although the quantitative differences between deflection curves for various η values appear subtle, a systematic analysis reveals that increasing the deformation parameter generally reduces the magnitude of deflection, particularly at intermediate velocities. This behavior suggests that the modified geometry introduces correction terms that partially counteract the gravitational attraction experienced by massive particles, potentially offering an observational signature of deformed spacetime structure.

Figure 9 complements this analysis by depicting the deflection angle as a function of impact parameter b for various velocity values v, maintaining $M = m = 1$. The results demonstrate that for all velocities, the deflection angle exhibits a characteristic inverse relationship with impact parameter, with stronger deflection occurring for trajectories passing closer to the BH. However, the magnitude of this effect varies significantly with velocity, with slower particles exhibiting systematically larger deflection angles across all impact parameters. This behavior reflects the fundamental difference between massive and massless particle dynamics in curved spacetime, where particles with lower velocities remain within the gravitational field for longer durations, accumulating greater deflection effects.

The velocity-dependent deflection patterns revealed by our analysis have significant implications for astrophysical observations. While direct detection of massive particle deflection presents greater observational challenges than electromagnetic lensing, potential applications exist in contexts such as cosmic ray propagation, neutrino astronomy, and dark matter distribution studies. The distinctive velocity dependence of deflection angles could potentially serve as a probe of both the deformation parameter η and the underlying gravitational field structure in regions where modified gravity effects might become significant.

This comprehensive analysis demonstrates that the Jacobi geometry approach provides a powerful theoretical framework for investigating massive particle dynamics in modified gravity scenarios. By reformulating the deflection problem in terms of an effective spatial geometry, we have established analytical expressions that quantify how both the deformation parameter η and particle velocity v influence gravitational deflection.

VIII. QUANTUM-CORRECTED THERMODYNAMICS OF SKZ BHs

The thermodynamic behavior of BHs represents a fundamental bridge between gravitational physics and quantum field theory, providing essential insights into the microscopic structure of spacetime [69, 70]. While classical BH thermodynamics has been extensively developed within the framework of general relativity, quantum corrections introduce significant modifications that manifest particularly in the entropy-area relationship [71, 72]. This section systematically investigates how the exponential correction (EC) entropy formalism modifies the thermodynamic properties of SKZ BHs, elucidating the interplay between quantum effects and the deformation parameter η.

The quantum-mechanical modifications to BH thermodynamics arise primarily from fluctuations in the quantum gravitational field, necessitating corrections to the classical Bekenstein-Hawking entropy formula [73]. These corrections are particularly significant in extreme regimes where semiclassical approximations become inadequate, potentially revealing signatures of underlying quantum gravity theories [74–77]. Within the EC entropy framework, we systematically incorporate quantum effects while maintaining analytical tractability, enabling rigorous examination of how fundamental thermodynamic quantities respond to both quantum fluctuations and geometric deformations.

The EC entropy formalism extends the standard Bekenstein-Hawking relation through the incorporation of quantum corrections in exponential form:

$$S = S_0 + \zeta e^{-S_0}, \tag{68}$$

where S_0 denotes the classical Bekenstein-Hawking entropy, defined as $S_0 = \frac{A_H}{4}$ with A_H representing the area of the event horizon. The correction term ζe^{-S_0}, governed by the parameter ζ, systematically incorporates quantum modifications to the entropy-area relationship, capturing leading-order quantum gravitational effects.

To determine the internal energy of the BH under EC entropy, we integrate the Hawking temperature T_H with respect to the entropy differential:

$$E_{EC} = \int T_H dS. \tag{69}$$

This formulation provides a quantum-corrected energy expression that accounts for both the geometric deformation characterized by η and the quantum corrections encoded in the EC entropy formalism:

$$E_{EC} \approx -\frac{M\pi r_h^2}{4} - \frac{3\eta\pi}{4} \ln r_h \tag{70}$$

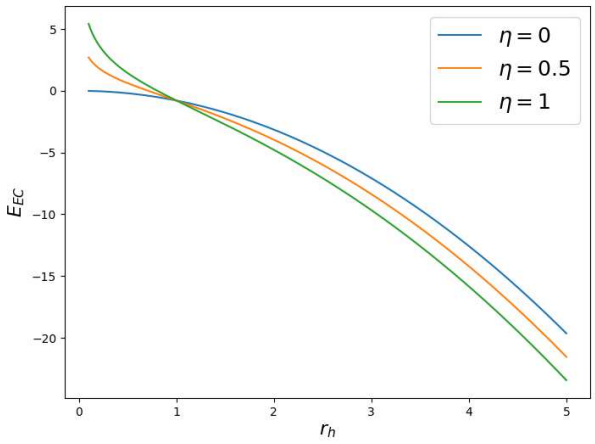

FIG. 10: Variation of exponentially corrected energy E_{EC} versus event horizon radius r_h for different values of the deformation parameter η. The plot demonstrates that quantum corrections significantly modify the energy profile, particularly for small BHs, with $\eta > 0$ creating regions of positive energy that indicate potential repulsive effects in the quantum-corrected gravitational field.

Figure 10 illustrates the functional relationship between the quantum-corrected internal energy E_{EC} and the event horizon radius r_h across different values of the deformation parameter η. This visualization reveals several critical features of how quantum corrections and geometric deformations collectively influence BH energetics. For small r_h values, particularly when $\eta > 0$, the internal energy exhibits positive values, contrasting with the negative energy states characteristic of classical BHs. This positivity potentially indicates the emergence of repulsive quantum gravitational effects that counteract the classical gravitational attraction at small length scales.

As the horizon radius increases, E_{EC} transitions to increasingly negative values, asymptotically approaching the classical behavior for large BHs where quantum effects become negligible. The systematic shift in energy curves with increasing η demonstrates that the deformation parameter intensifies the rate at which the internal energy decreases with increasing radius, suggesting that geometric deformations amplify the energetic consequences of quantum corrections. This coupling between deformation and quantum effects creates distinct thermodynamic regimes that differ qualitatively from both classical Schwarzschild BHs and non-deformed quantum-corrected BHs.

The Helmholtz free energy F_{EC} represents another fundamental thermodynamic potential that quantifies the energy available for conversion to work under conditions of constant temperature. This quantity, directly related to the EC entropy, is formulated as:

$$F_{EC} = -\int S dT_H. \tag{71}$$

To investigate the impact of EC entropy on the Helmholtz free energy, we express the entropy function as a Taylor expansion up to second-order. Consequently, we obtain:

$$F_{EC} \approx -\frac{M}{2\pi r_h^2} - \frac{9\eta}{16\pi r_h^4} - \frac{M\pi r_h^2}{4} - \frac{9\eta\pi}{8} \ln r_h \tag{72}$$

Figure 11 depicts the functional dependence of the quantum-corrected Helmholtz free energy F_{EC} on the event horizon radius r_h for various deformation parameter values. The analysis reveals that for small BHs (small r_h values), particularly when $\eta > 0$, the free energy exhibits a rapid decline to negative values. This behavior signifies that quantum corrections fundamentally alter the thermodynamic stability landscape, potentially enhancing evaporation processes for microscopic BHs. The systematic dependence on the deformation parameter demonstrates that as η increases, the negative energy contributions become more pronounced, suggesting that geometrically deformed BHs experience intensified quantum corrections to their thermodynamic properties.

For larger BHs (increasing r_h), F_{EC} asymptotically approaches zero, signifying a progressive return to classical thermodynamic behavior as quantum effects become increasingly negligible. This convergence pattern confirms that quantum corrections primarily influence small-scale BH behavior, while large BHs remain effectively described by classical thermodynamics. The comparative analysis across different η values reveals that small deformation parameters produce thermodynamic profiles relatively close to standard Schwarzschild behavior, while larger deformations generate more substantial deviations

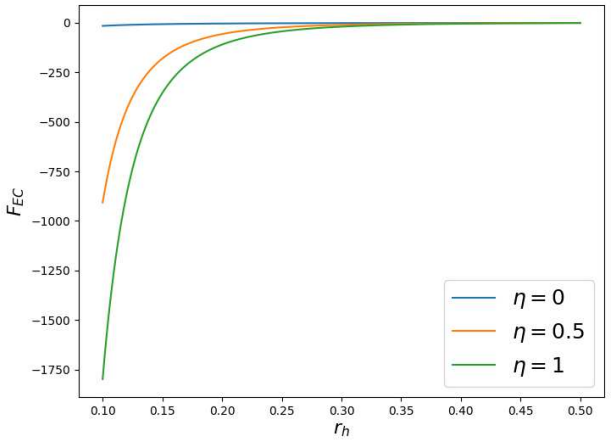

FIG. 11: Helmholtz free energy F_{EC} as a function of the event horizon radius r_h for different values of the deformation parameter η, with mass parameter fixed at $M = 1$. The plot reveals that quantum corrections induce rapid decreases in free energy for small BHs, with the effect amplified by increasing η values, indicating enhanced thermodynamic instability in the quantum-corrected regime.

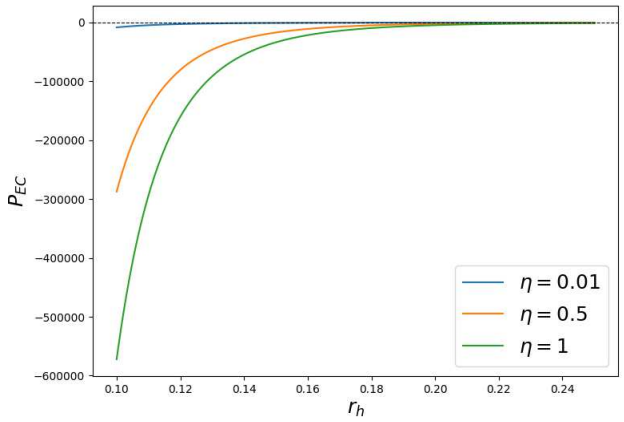

FIG. 12: Quantum-corrected pressure P_{EC} as a function of the event horizon radius r_h for different values of the deformation parameter η, with mass parameter fixed at $M = 1$. The consistently negative pressure values indicate inward-directed thermodynamic forces that intensify with increasing η, particularly for small BHs where quantum effects dominate.

from classical predictions, particularly in the small-r_h regime where quantum effects predominate.

The pressure P_{EC} of the system represents the force per unit area exerted by the BH on its surroundings and connects to the free energy through the thermodynamic relation:

$$P_{EC} \approx -\frac{dF_{EC}}{dV}, \tag{73}$$

where V denotes the volume enclosed by the event horizon. By differentiating the free energy expression, we determine the quantum-corrected pressure for the SKZ BH as:

$$P_{EC} \approx -\frac{M}{4\pi^2 r_h^5} - \frac{9\eta}{16\pi^2 r_h^7} + \frac{M}{8} + \frac{9\eta}{32 r_h^3} \tag{74}$$

Figure 12 illustrates the quantum-corrected pressure P_{EC} as a function of event horizon radius r_h for various deformation parameter values. The consistently negative pressure values at small r_h indicate that the thermodynamic system experiences an inward-directed force, consistent with gravitational contraction. This negative pressure regime becomes particularly pronounced for small BHs, where quantum corrections exert their strongest influence. The systematic dependence on η demonstrates that increasing the deformation parameter intensifies the negative pressure magnitude, suggesting that geometrically deformed spacetimes experience enhanced contractive thermodynamic forces under quantum corrections.

As the horizon radius increases, P_{EC} asymptotically approaches zero, indicating a diminishing thermodynamic pressure for large BHs where both quantum effects and geometric deformations become increasingly negligible relative to classical gravity. The absence of positive pressure regimes across all parameter values suggests that quantum corrections predominantly reinforce rather than counteract the contractive nature of BH thermodynamics, even when geometric deformations are substantial. This behavior indicates that EC entropy modifications primarily influence the magnitude rather than the directional character of thermodynamic forces in BH systems.

Finally, we analyze the specific heat capacity C_{EC}, a critical parameter that quantifies how the BH's temperature responds to changes in entropy. This quantity, defined as:

$$C_{EC} = T_H \left(\frac{\partial S_{EC}}{\partial T_H} \right), \tag{75}$$

provides essential insights into thermodynamic stability and phase structure. From this definition, we derive:

$$C_{EC} \approx \frac{4\pi^2 r_h^4 \left(M r_h^2 + \frac{3\eta}{2} \right)}{4M r_h^2 + 9\eta} \tag{76}$$

Figure 13 presents the quantum-corrected heat capacity C_{EC} as a function of the event horizon radius r_h for various deformation parameter values. The analysis reveals that C_{EC} exhibits consistently positive values

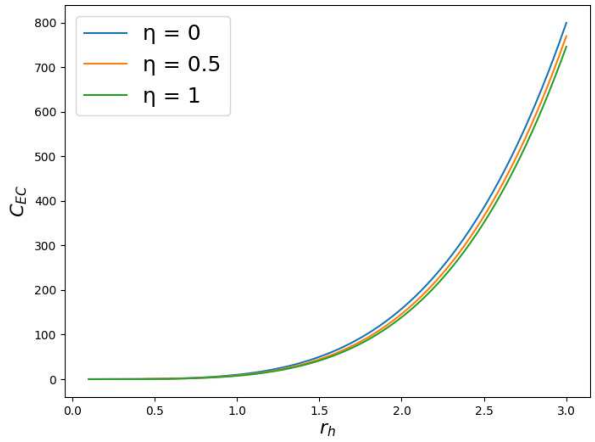

FIG. 13: Specific heat capacity C_{EC} as a function of the event horizon radius r_h for different values of the deformation parameter η, with mass parameter fixed at $M = 1$. The consistently positive heat capacity indicates thermodynamic stability across all parameter regimes, though higher η values slightly reduce the heat capacity magnitude, potentially altering evaporation dynamics.

that increase monotonically with r_h, indicating thermodynamic stability across all parameter regimes. This continuous positive behavior contrasts with the heat capacity discontinuities characteristic of certain classical BH solutions, suggesting that quantum corrections potentially regularize thermodynamic behavior by eliminating phase transitions.

The systematic influence of the deformation parameter manifests as a subtle modulation of the heat capacity magnitude, with larger η values slightly reducing C_{EC} at comparable horizon radii. This reduced heat capacity indicates that geometrically deformed BHs exhibit modestly diminished thermal responsiveness, potentially altering evaporation dynamics and equilibration processes. The absence of singularities, discontinuities, or sign changes in the heat capacity curves confirms that quantum-corrected SKZ BHs maintain thermodynamic stability throughout their evolution, regardless of the deformation parameter magnitude.

IX. CONCLUSION

In this study, we conducted a comprehensive investigation of deformed BH geometries through the SKZ metric, systematically analyzing how parametric deviations from the standard Schwarzschild solution manifest across multiple physical domains. The introduction of the deformation parameter η enabled us to quantitatively track modifications to both the thermodynamic behavior and gravitational lensing characteristics, thereby establishing a theoretical framework for constraining potential departures from GR through astrophysical observations.

Our analysis of the SKZ BH geometry in Sec. II revealed that the parameter η fundamentally alters the event horizon structure, producing BHs with identical ADM mass but different horizon radii—a distinctive feature with significant thermodynamic implications. We identified a critical threshold $\eta_{\min} = -32/27M^3$ below which the spacetime would violate the cosmic-censorship conjecture, establishing theoretical constraints on the permissible parameter range. The computation of Hawking temperature demonstrated that positive deformation parameters induce increased thermal radiation, particularly pronounced for small BHs, as visualized in Figure 1.

The perturbative analysis of gravitational lensing conducted in Sec. III yielded analytical expressions for the deflection angle of light in SKZ spacetime. By solving the differential equation (18) through a systematic power series expansion, we derived closed-form expressions showing how η introduces higher-order corrections to the standard Schwarzschild lensing formula. The resulting deflection angle, expressed in Eq. 28, revealed that the deformation parameter contributes terms proportional to b^{-3}, providing a potential observational signature for testing modified gravity theories through precision lensing measurements. Our examination of magnification properties in Sec. IV extended this analysis to the observational domain, demonstrating how the deformation parameter systematically modifies the position and amplitude of magnification peaks, particularly in the radial component μ_{rad}. The comparative visualization in Figure 4 illustrated that SKZ BHs with substantial deformation parameters generate distinctive magnification profiles that could potentially be detected through microlensing observations. This finding establishes magnification signatures as a promising observational probe for constraining deviations from standard Schwarzschild geometry.

The application of topological methods in Sec. V, specifically the GB theorem, provided an elegant alternative approach to computing deflection angles. This method yielded an expression for the deflection angle (28) that incorporated corrections due to the deformation parameter, with the dependence on impact parameter visualized in Fig. 5. The results demonstrated enhanced gravitational lensing effects for increasing values of η, particularly at small impact parameters, confirming the potential observational significance of the deformation parameter in strong-field lensing scenarios. Section VI extended our analysis to include plasma effects, revealing how frequency-dependent refractive properties couple with the underlying deformed geometry to produce chromatic lensing signatures. The derived expression for the plasma-modified deflection angle (Eq. 56) demonstrated that plasma enhances the gravitational lensing effect, with higher plasma densities significantly increasing the deflection angle, particularly at small impact pa-

rameters, as illustrated in Figs. 6 and 7. These results established that multi-frequency observations of gravitationally lensed sources could potentially reveal signatures of the deformation parameter, offering a novel observational probe of modified gravity theories.

Our investigation of massive particle dynamics in Sec. VII through the Jacobi metric approach revealed how velocity-dependent corrections manifest in the gravitational deflection of non-relativistic particles. The analytical expression for the deflection angle demonstrated a complex dependence on both the deformation parameter and particle velocity, with particularly pronounced effects for slow-moving particles. Figures 8 and 9 visualized this velocity dependence, showing that particles with lower velocities experience significantly greater deflection than those approaching the speed of light, with the deformation parameter introducing subtle modifications to this behavior. These findings extended the standard lensing formalism beyond null geodesics, providing a theoretical framework for understanding how modified gravity theories might influence massive particle trajectories.

The examination of quantum-corrected thermodynamics in Sec. VIII employed the exponential correction EC entropy formalism to analyze how quantum effects modify the thermodynamic properties of SKZ BHs. Our calculations revealed that the interplay between quantum corrections and the deformation parameter generates distinctive thermodynamic signatures, particularly for small BHs where quantum effects predominate. The internal energy profile (Figure 10) demonstrated that quantum corrections and positive deformation parameters can induce regions of positive energy, potentially indicating repulsive effects that counteract classical gravitational attraction. Similarly, the Helmholtz free energy (Figure 11) exhibited rapid declines for small BHs with increasing deformation parameters, suggesting enhanced thermodynamic instability in the quantum-corrected regime. Despite these modifications, the heat capacity remained consistently positive across all parameter regimes (Figure 13), indicating that quantum-corrected SKZ BHs maintain thermodynamic stability throughout their evolution.

The systematic analysis conducted throughout this investigation demonstrated that the deformation parameter η introduces significant modifications to both gravitational lensing phenomena and thermodynamic behavior, with particularly pronounced effects in strong-field regimes and for small BHs where quantum corrections become significant. These modifications potentially offer multiple observational signatures for testing deviations from standard GR, including enhanced deflection angles, distinctive magnification patterns, chromatic plasma effects, and modified thermodynamic properties. The mathematical framework developed in this study provides a foundation for quantitatively constraining such deviations through precision astrophysical measurements. Extending our analysis to rotating BHs through the incorporation of spin parameters would provide a more comprehensive framework for testing modified gravity theories against astrophysical observations. Second, investigating potential quantum gravity mechanisms like GUP [78–80] KZ BHs that might provide deeper theoretical insights into the deformed BH radiation. These research directions collectively offer promising pathways for further bridging theoretical models of modified gravity with observational astrophysics.

ACKNOWLEDGMENTS

We thank EMU, TÜBİTAK, ANKOS, and SCOAP3 for academic and/or finacial support. İ. S. also acknowledges the networking support from COST Actions CA22113, CA21106, and CA23130.

[1] Stephen W. Hawking and George F. R. Ellis, *The Large Scale Structure of Space-Time*, Cambridge Monographs on Mathematical Physics (Cambridge University Press, 2023).

[2] Don N Page, "Black hole information," in *Proceedings of the 5th Canadian conference on general relativity and relativistic astrophysics*, Vol. 1 (World Scientific, 1994) pp. 1–41.

[3] Tanmay Vachaspati, Dejan Stojkovic, and Lawrence M Krauss, "Observation of incipient black holes and the information loss problem," Physical Review D—Particles, Fields, Gravitation, and Cosmology **76**, 024005 (2007).

[4] Mehdi El Bouhaddouti and Ilias Cholis, "On the mass distribution of the ligo-virgo-kagra events," Physical Review D **111**, 043020 (2025).

[5] Aditya Vijaykumar, Maya Fishbach, Susmita Adhikari, and Daniel E Holz, "Inferring host-galaxy properties of ligo–virgo–kagra's black holes," The Astrophysical Journal **972**, 157 (2024).

[6] Andrea Antonelli, Konstantinos Kritos, Ken KY Ng, Roberto Cotesta, and Emanuele Berti, "Classifying the generation and formation channels of individual ligo-virgo-kagra observations from dynamically formed binaries," Physical Review D **108**, 084044 (2023).

[7] Roman Konoplya, Luciano Rezzolla, and Alexander Zhidenko, "General parametrization of axisymmetric black holes in metric theories of gravity," Physical Review D **93**, 064015 (2016).

[8] Yixuan Ma and Luciano Rezzolla, "Horizon-penetrating form of parametrized metrics for static and stationary black holes," Physical Review D **110**, 024032 (2024).

[9] Renan B Magalhães, Luiz CS Leite, and Luís CB Crispino, "Absorption by deformed black holes," Physics Letters B **805**, 135418 (2020).

[10] Sourabh Nampalliwar, Shuo Xin, Shubham Srivastava, Askar B Abdikamalov, Dimitry Ayzenberg, Cosimo Bambi, Thomas Dauser, Javier A Garcia, and Ashutosh Tripathi, "Testing general relativity with x-ray re-

flection spectroscopy: The konoplya-rezzolla-zhidenko parametrization," Physical Review D **102**, 124071 (2020).
[11] Joachim Wambsganss, "Gravitational lensing in astronomy," Living Reviews in Relativity **1**, 1–74 (1998).
[12] Oğuzhan Kaşıkçı and Cemsinan Deliduman, "Gravitational lensing in weyl gravity," Physical Review D **100**, 024019 (2019).
[13] Erdem Sucu and İzzet Sakallı, "Dynamics of particles surrounding a stationary, spherically-symmetric black hole with nonlinear electrodynamics," Physics of the Dark Universe **47**, 101771 (2025).
[14] Pedro VP Cunha and Carlos AR Herdeiro, "Shadows and strong gravitational lensing: a brief review," General Relativity and Gravitation **50**, 1–27 (2018).
[15] Roger D Blandford and Ramesh Narayan, "Cosmological applications of gravitational lensing," In: Annual review of astronomy and astrophysics. Vol. 30 (A93-25826 09-90), p. 311-358. **30**, 311–358 (1992).
[16] Kimet Jusufi and Ali Övgün, "Gravitational lensing by rotating wormholes," Physical Review D **97**, 024042 (2018).
[17] Shangyun Wang, Songbai Chen, and Jiliang Jing, "Strong gravitational lensing by a konoplya-zhidenko rotating non-kerr compact object," Journal of Cosmology and Astroparticle Physics **2016**, 020 (2016).
[18] Fen Long, Songbai Chen, Shangyun Wang, and Jiliang Jing, "Energy extraction from a konoplya–zhidenko rotating non-kerr black hole," Nuclear Physics B **926**, 83–94 (2018).
[19] Jean-Paul Kneib and Priyamvada Natarajan, "Cluster lenses," The Astronomy and Astrophysics Review **19**, 1–100 (2011).
[20] Tommaso Treu and Richard S Ellis, "Gravitational lensing: Einstein's unfinished symphony," Contemporary Physics **56**, 17–34 (2015).
[21] Renan B Magalhães, Luiz CS Leite, and Luís CB Crispino, "Parametrized black holes: scattering investigation," The European Physical Journal C **82**, 698 (2022).
[22] Zhonghua Li, "Note on the corrected hawking temperature of a parametric deformed black hole with influence of quantum gravity," Advances in High Energy Physics **2023**, 9702181 (2023).
[23] Karlo de Leon and Ian Vega, "Weak gravitational deflection by two-power-law densities using the gauss-bonnet theorem," Physical Review D **99**, 124007 (2019).
[24] Erdem Sucu and Ali Övgün, "The effect of quark–antiquark confinement on the deflection angle by the ned black hole," Physics of the Dark Universe **44**, 101446 (2024).
[25] Gabriel Crisnejo and Emanuel Gallo, "Weak lensing in a plasma medium and gravitational deflection of massive particles using the gauss-bonnet theorem. a unified treatment," Physical Review D **97**, 124016 (2018).
[26] Yashmitha Kumaran and Alï Övgün, "Deriving weak deflection angle by black holes or wormholes usinggauss-bonnet theorem," Turkish Journal of Physics **45**, 247–267 (2021).
[27] Volker Perlick, "Gravitational lensing from a spacetime perspective," Living reviews in relativity **7**, 1–117 (2004).
[28] AO Petters and MC Werner, "Mathematics of gravitational lensing: multiple imaging and magnification," General Relativity and Gravitation **42**, 2011–2046 (2010).
[29] Chenni Xu and Li-Gang Wang, "Theory of light propagation in arbitrary two-dimensional curved space," Photonics Research **9**, 2486–2493 (2021).
[30] Gennady S Bisnovatyi-Kogan and Oleg Yu Tsupko, "Gravitational lensing in presence of plasma: strong lens systems, black hole lensing and shadow," Universe **3**, 57 (2017).
[31] Ali Övgün, "Weak gravitational lensing in Ricci-coupled Kalb–Ramond bumblebee gravity: Global monopole and axion-plasmon medium effects," Phys. Dark Univ. **48**, 101905 (2025).
[32] Gennady S Bisnovatyi-Kogan and Oleg Yu Tsupko, "Time delay induced by plasma in strong lens systems," Monthly Notices of the Royal Astronomical Society **524**, 3060–3067 (2023).
[33] Francesco Comberiati and Leonardo de la Cruz, "Gravitational lensing in a plasma from worldlines," Physical Review D **111**, 054030 (2025).
[34] Jonas R Mureika, John W Moffat, and Mir Faizal, "Black hole thermodynamics in modified gravity (mog)," Physics Letters B **757**, 528–536 (2016).
[35] Ganim Gecim and Yusuf Sucu, "Quantum gravity effect on the tunneling particles from warped-ads3 black hole," Modern Physics Letters A **33**, 1850164 (2018).
[36] E Sucu and İ Sakallı, "Gup-reinforced hawking radiation in rotating linear dilaton black hole spacetime," Physica Scripta **98**, 105201 (2023).
[37] Jacob D Bekenstein, "Black holes and entropy," Physical Review D **7**, 2333 (1973).
[38] Gilad Lifschytz and Miguel Ortiz, "Black hole thermodynamics from quantum gravity," Nuclear Physics B **486**, 131–148 (1997).
[39] Wajiha Javed, Mehak Atique, and Ali Övgün, "Probing effective loop quantum gravity on weak gravitational lensing, hawking radiation and bounding greybody factor by black holes," General Relativity and Gravitation **54**, 135 (2022).
[40] Ganim Gecim and Yusuf Sucu, "Quantum gravity correction to hawking radiation of the 2+ 1-dimensional wormhole," Advances in High Energy Physics **2020**, 7516789 (2020).
[41] Wajiha Javed, Riasat Ali, Rimsha Babar, and Ali Övgün, "Tunneling of massive vector particles under influence of quantum gravity," Chinese Physics C **44**, 015104 (2020).
[42] Behnam Pourhassan, "Exponential corrected thermodynamics of black holes," Journal of Statistical Mechanics: Theory and Experiment **2021**, 073102 (2021).
[43] Erdem Sucu and İzzet Sakallı, "Exploring lorentz-violating effects of kalb-ramond field on charged black hole thermodynamics and photon dynamics," Physical Review D **111**, 064049 (2025).
[44] Roman Konoplya and Alexander Zhidenko, "Detection of gravitational waves from black holes: Is there a window for alternative theories?" Physics Letters B **756**, 350–353 (2016).
[45] Clifford M Will, "The confrontation between general relativity and experiment," Living reviews in relativity **17**, 1–117 (2014).
[46] Bruno Bertotti, Luciano Iess, and Paolo Tortora, "A test of general relativity using radio links with the cassini

spacecraft," Nature **425**, 374–376 (2003).
[47] James G Williams, Slava G Turyshev, and Dale H Boggs, "Progress in lunar laser ranging tests of relativistic gravity," Physical Review Letters **93**, 261101 (2004).
[48] Ibrahima Bah and Pierre Heidmann, "Geometric resolution of the schwarzschild horizon," Physical Review D **109**, 066014 (2024).
[49] Jop Briet and David Hobill, "Determining the Dimensionality of Spacetime by Gravitational Lensing," (2008), arXiv:0801.3859 [gr-qc].
[50] Paul AM Dirac, "The lagrangian in quantum mechanics," in *Feynman's Thesis—A New Approach To Quantum Theory* (World Scientific, 2005) pp. 111–119.
[51] "webbtelescope.org," (2018).
[52] Xu Lu and Yi Xie, "Gravitational lensing by a quantum deformed schwarzschild black hole," The European Physical Journal C **81**, 1–19 (2021).
[53] KS Virbhadra, "Relativistic images of schwarzschild black hole lensing," Physical Review D—Particles, Fields, Gravitation, and Cosmology **79**, 083004 (2009).
[54] "hubblesite.org," (2022).
[55] Margarita Safonova, Diego F Torres, and Gustavo E Romero, "Microlensing by natural wormholes: theory and simulations," Physical Review D **65**, 023001 (2001).
[56] Jitendra Kumar, Shafqat Ul Islam, and Sushant G Ghosh, "Investigating strong gravitational lensing effects by supermassive black holes with horndeski gravity," The European Physical Journal C **82**, 443 (2022).
[57] Kumar Shwetketu Virbhadra and George FR Ellis, "Schwarzschild black hole lensing," Physical Review D **62**, 084003 (2000).
[58] Erik Zackrisson, Adi Zitrin, Michele Trenti, Claes-Erik Rydberg, Lucia Guaita, Daniel Schaerer, Tom Broadhurst, Göran Östlin, and Tina Ström, "Detecting gravitationally lensed population iii galaxies with the hubble space telescope and the james webb space telescope," Monthly Notices of the Royal Astronomical Society **427**, 2212–2223 (2012).
[59] Raúl Carballo-Rubio, Vitor Cardoso, and Ziri Younsi, "Toward very large baseline interferometry observations of black hole structure," Physical Review D **106**, 084038 (2022).
[60] Hideyoshi Arakida, "The optical geometry definition of the total deflection angleof a light ray in curved spacetime," Journal of Cosmology and Astroparticle Physics **2021**, 028 (2021).
[61] Oleg Yu Tsupko and Gennady S Bisnovatyi-Kogan, "Gravitational lensing in plasma: Relativistic images at homogeneous plasma," Physical Review D—Particles, Fields, Gravitation, and Cosmology **87**, 124009 (2013).
[62] Volker Perlick, Oleg Yu. Tsupko, and Gennady S. Bisnovatyi-Kogan, "Influence of a plasma on the shadow of a spherically symmetric black hole," Phys. Rev. D **92**, 104031 (2015), arXiv:1507.04217 [gr-qc].
[63] G. S. Bisnovatyi-Kogan and O. Yu. Tsupko, "Gravitational lensing in a non-uniform plasma," Mon. Not. Roy. Astron. Soc. **404**, 1790–1800 (2010), arXiv:1006.2321 [astro-ph.CO].
[64] Zonghai Li and Junji Jia, "The finite-distance gravitational deflection of massive particles in stationary spacetime: a jacobi metric approach," The European Physical Journal C **80**, 157 (2020).
[65] Zonghai Li and Ali Övgün, "Finite-distance gravitational deflection of massive particles by a kerr-like black hole in the bumblebee gravity model," Physical Review D **101**, 024040 (2020).
[66] GW Gibbons, "The jacobi metric for timelike geodesics in static spacetimes," Classical and Quantum Gravity **33**, 025004 (2015).
[67] Marcos Argañaraz and Oscar Lasso Andino, "Dynamics in wormhole spacetimes: a jacobi metric approach," Classical and Quantum Gravity **38**, 045004 (2020).
[68] Zonghai Li and Junji Jia, "Kerr-newman-jacobi geometry and the deflection of charged massive particles," Physical Review D **104**, 044061 (2021).
[69] Dieter Lüst and Ward Vleeshouwers, *Black hole information and thermodynamics*, Tech. Rep. (Springer, 2019).
[70] Robert M Wald, "The thermodynamics of black holes," Living reviews in relativity **4**, 1–44 (2001).
[71] Shahar Hod, "High-order corrections to the entropy and area of quantum black holes," Classical and Quantum Gravity **21**, L97 (2004).
[72] Abhishek Pathak, Achilleas P Porfyriadis, Andrew Strominger, and Oscar Varela, "Logarithmic corrections to black hole entropy from kerr/cft," Journal of High Energy Physics **2017**, 1–14 (2017).
[73] AA Bytsenko and AJNP Tureanu, "Quantum corrections to bekenstein–hawking black hole entropy and gravity partition functions," Nuclear Physics B **873**, 534–549 (2013).
[74] R Alves Batista, G Amelino-Camelia, D Boncioli, JM Carmona, A Di Matteo, G Gubitosi, I Lobo, NE Mavromatos, C Pfeifer, D Rubiera-Garcia, *et al.*, "White paper and roadmap for quantum gravity phenomenology in the multi-messenger era," Classical and quantum gravity **42**, 032001 (2025).
[75] D. Amati, M. Ciafaloni, and G. Veneziano, "Classical and Quantum Gravity Effects from Planckian Energy Superstring Collisions," Int. J. Mod. Phys. A **3**, 1615–1661 (1988).
[76] Nima Arkani-Hamed, Savas Dimopoulos, and G. R. Dvali, "Phenomenology, astrophysics and cosmology of theories with submillimeter dimensions and TeV scale quantum gravity," Phys. Rev. D **59**, 086004 (1999), arXiv:hep-ph/9807344.
[77] Ganim Gecim and Yusuf Sucu, "Quantum gravity effect on the hawking radiation of spinning dilaton black hole," The European Physical Journal C **79**, 1–9 (2019).
[78] A Bina, S Jalalzadeh, and A Moslehi, "Quantum black hole in the generalized uncertainty principle framework," Physical Review D—Particles, Fields, Gravitation, and Cosmology **81**, 023528 (2010).
[79] Ana Alonso-Serrano, Mariusz P Dabrowski, and Hussain Gohar, "Generalized uncertainty principle impact onto the black holes information flux and the sparsity of hawking radiation," Physical Review D **97**, 044029 (2018).
[80] Ganim Gecim and Yusuf Sucu, "Quantum gravity effect on the hawking radiation of charged rotating btz black hole," General Relativity and Gravitation **50**, 1–15 (2018).